Evolving Structures in Complex Systems

Hugo Cisneros
CIIRC, CTU in Prague[1]
ENS Paris-Saclay
hugo.cisneros@ens-paris-saclay.fr

Josef Sivic
Inria, DI-ENS, PSL[2]
CIIRC, CTU in Prague[1]
josef.sivic@inria.fr

Tomas Mikolov
Facebook AI
tmikolov@fb.com

Abstract—In this paper we propose an approach for measuring growth of complexity of emerging patterns in complex systems such as cellular automata. We discuss several ways how a metric for measuring the complexity growth can be defined. This includes approaches based on compression algorithms and artificial neural networks. We believe such a metric can be useful for designing systems that could exhibit open-ended evolution, which itself might be a prerequisite for development of general artificial intelligence. We conduct experiments on 1D and 2D grid worlds and demonstrate that using the proposed metric we can automatically construct computational models with emerging properties similar to those found in the Conway's Game of Life, as well as many other emergent phenomena. Interestingly, some of the patterns we observe resemble forms of artificial life. Our metric of structural complexity growth can be applied to a wide range of complex systems, as it is not limited to cellular automata.

I. INTRODUCTION

Recent advances in machine learning and deep learning have had successes at reproducing some very complex feats traditionally thought to be only achievable by living beings. However, making these systems adaptable and capable of developing and evolving on their own remains a challenge that might be crucial for eventually developing AI with general learning capabilities (for example as is further discussed in [1]). Building systems that mimic some key aspects of the behavior of existing intelligent organisms (such as the ability to evolve, improve, adapt, etc.) might represent a promising path. Intelligent organisms — e.g., human beings but also most living organisms if we consider a broad definition of intelligence — are a form of spontaneously occurring, ever evolving complex systems that exhibit these kinds of properties [2]. The ability to sustain open-ended evolution appears to be a requirement in order to enable emergence of arbitrarily complex adaptive systems.

Although a rigorous attempt at defining intelligence or life is beyond the scope of this paper, we assume that a system we might identify as evolving, with the potential of developing intelligence, should have the property of self-preservation and the ability to grow in complexity over time. These properties can be observed in living organisms [2] and should also be a part of computational models that aim to mimic them.

[1]CIIRC - Czech Institute of Informatics, Robotics and Cybernetics, Czech Technical University in Prague.

[2]WILLOW project, Departement d'Informatique de l'École Normale Supérieure, ENS/INRIA/CNRS UMR 8548, PSL Research University.

To recognize self-preservation and growth in complexity, one should be able to detect emerging macro-structures composed of smaller elementary components. For the purpose of obtaining computational models that grow in complexity over time, one should also be able to determine the amount of complexity these systems contain. We propose and discuss in this paper several ways of estimating the complexity and detecting the presence of emerging and stable patterns in complex systems such as cellular automata. We show that such metrics are useful when searching the space of cellular automata with the objective of finding those that seem to evolve in time.

II. RELATED WORK

A. Artificial life and open-ended evolution

Several works have attempted to artificially create open-ended evolution. A non-exhaustive list of some well known systems include Tierra [3], Sims [4], Avida [5], Polyworld [6], Geb [7], Division Blocks [8] and Chromaria [9]. Designs focusing on an objective, and making use of reinforcement learning methods to drive evolution are also being studied, e.g. in [10]. Most of these simulated "worlds" have had some success in reproducing key aspects of evolving artificial life, enabling the emergence of complex behavior from simple organisms. However, they still work within constrained simulated environments and usually consider organisms composed of elementary building blocks, while they don't work outside of this usually very constrained framework. Divergent and creative evolutionary process could be happening at a much lower conceptual level with fewer assumptions. For this reason, we consider cellular automata in the rest of the paper because they rely on a very few assumptions while offering a very large expressive power and a potentially wide range of behaviors that can be discovered. However, the metrics defined in this paper have the potential to be applied to other types of complex systems as discussed in Section VII.

B. Cellular automata

Cellular automata are very simple systems, usually defined in one or two dimensions, composed of cells that can be in a set of states. The cells are updated in discrete time steps using a transition table that defines the next state of a cell given the states of its neighbors. They were originally proposed by Stanislaw Ulam and studied by Von Neumann [11], who was interested in designing a computational system

that can self-reproduce itself in a non-trivial way. The trivial self-reproducing patterns were then those that do not have potential to evolve, for example the growth of crystals.

Stephen Wolfram later took a more bottom up approach, beginning with the study of the simple 1D binary cellular automata (CA), and identifying four qualitative classes of cellular automaton behavior [12]:

Class 1 evolves to a homogeneous state.
Class 2 evolves to simple periodic patterns.
Class 3 yields aperiodic disordered patterns.
Class 4 yields complex aperiodic and localized structures, including propagating structures.

Wolfram and his colleagues also studied 2D CA using tools from information theory and dynamical systems theory, describing the global properties of these systems in terms of entropies and Lyapunov exponents [13].

Christopher Langton and colleagues also studied CA dynamics [14] — e.g. using the λ parameter [15] — and designed a self-replicating pattern much simpler than Von Neumann's [16], now known as Langton's loops. The main issues with his system and Von Neumann's universal replicator is the fact that they are very fragile and based on a large amount of human design. As a consequence, although they do self-replicate, they cannot increase in complexity and are not robust to perturbations or unexpected interactions with the environment.

A genetic algorithm-based search for spontaneously occurring self-replicating patterns in 2D cellular automata with several states was undertaken in [17] using entropy measures of the frequency distribution of 3×3 patterns.

C. Compression and complexity

Compression has often been used as a measure of complexity. Lempel and Ziv have introduced in [18] the now widespread Lempel-Ziv (LZ) algorithm as a method for measuring the complexity of a sequence. By constructing back-references to previous parts of a string, the LZ algorithm is capable of taking advantage of duplicate patterns in the input to reduce its size. The DEFLATE algorithm that we use in the following section combines LZ with Huffman coding for efficient representation of the symbols obtained after the first step. It is one of the most widespread compression algorithms and is for instance used in gzip and PNG file compression standards.

The PAQ compression algorithm series [19] is an ensemble of compression algorithms initially developed by Matt Mahoney with state of the art compression ratio on several compression benchmarks. Better compression of an input means a better approximation of the minimum description length and implicit understanding of more of the underlying patterns in input data. The usefulness of a better compressor is that it can detect much more complex and intricate patterns that aren't simple repetitions of previous patterns.

In [20], H. Zenil investigates the effects of a compression-based metric to classify cellular automata and observes that it results in a partitioning of the space of 1D CA into several clusters that match Wolfram's classes of automata.

He also used this approach on the output of simple Turing machines and some 1D automata with more than two states and larger neighborhoods. Extensions of this work include asymptotic sensitivity analysis of the compressed length for input configurations of growing complexity, as introduced in [21], [22].

Additionally, image decompression time as an approximation of Bennet's logical depth [23], [24] and the output distribution of simple Turing machines combined with block decomposition of CA to approximate their algorithmic complexity have also been investigated [25], [26]. However, the possible extent to which such measures of complexity could be applied to more complex automata and other complex systems has not yet been extensively studied. For a review of several measures of complexity and their applications, see [27].

III. COMPRESSION-BASED METRIC

A cellular automaton of size n in 1D can be represented at time t by its grid-state $S^{(t)} = \{c_1^{(t)}, ..., c_n^{(t)}\}$ where each c_i (also called a cell) can take one of k possible values (representing the possible states), and a transition rule ϕ. The transition rule is defined with respect to a neighborhood radius r with the mapping $\phi(c_{i-r}^{(t)}, ..., c_i^{(t)} ..., c_{i+r}^{(t)}) = c_i^{(t+1)}$ that maps $\{1, ..., k\}^{2r+1}$ to $\{1, ..., k\}$. The quantity $2r+1$ corresponds to the number of cells taken into account for computing the next state of a cell, namely that cell itself and r neighboring cells in both directions.

Simulating a CA amounts to the recursive application of this mapping ϕ to an initial state $S^{(0)} = \{c_1^{(0)}, ..., c_n^{(0)}\}$.

In the rest of the paper, we consider cyclic boundary conditions for the automata, meaning that the indices $i-r, ..., i+r$ above are taken modulo n the size of the automaton in 1D. Boundary conditions can have some effect on a CA's evolution, but cyclic boundaries have been empirically observed to have limited effect on the complexity of automata in 1D [28].

The definition given in the equation above can be extended to higher dimensional automata by modifying the neighborhood and the definition of ϕ. A 2D neighborhood of radius 1 can be defined as the 3 by 3 square around the center cell — also called the Moore neighborhood — or by only considering the four immediate horizontal and vertical neighbors of the center cell — the Von Neumann neighborhood.

Elementary cellular automata (ECA) are 1D CA with $k = 2$ and $r = 1$. There are 2^3 elements in $\{1, ..., k\}^{2r+1}$ and $2^{2^3} = 256$ possible different set transition rules that are often compactly represented as a binary string with 8 bits. The relatively low number of rules of this type makes it possible to appreciate the performance of a metric and compare it with others.

We define the compressed length C of a 1D cellular automaton at time t as

$$C(S^T) = \text{length}\left(\text{comp}(c_1 \mid\mid c_2 \mid\mid ... c_n)\right) \quad (1)$$

where $\mid\mid$ denotes the string concatenation operator and the cells c_i are implicitly converted into string characters (with one symbol per unique state). `comp` is a compression algorithm

(a) 6 highest scoring automata. Only the first 30 timesteps are shown for readability.
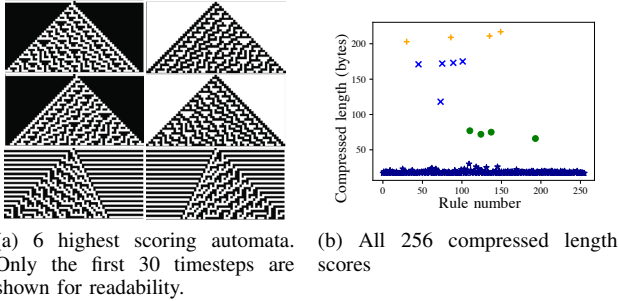
(b) All 256 compressed length scores

Fig. 1. Compression-based metric on 1D ECA. 1a represents the 1D ECA evolution with each line being the state of the automaton at a given timestep, starting from a single cell set to 1. Cells which are in state 1 are represented in black and cells in state 0 are represented in white. Time increases downwards. Figure 1b represents the compressed length of the 256 ECA rules, with different marker and colors corresponding to the obtained KMeans clusters.

that takes a string as input and outputs a compressed string, and length is the operator that returns the length of an input string.

Similarly to [29], [20], we use zlib's C implementation of DEFLATE to compress the final state of the automaton. If we apply the above metric to the 256 ECA run for 512 timesteps and initialized with one activated cell in the middle, we obtain the plot of Figure 1b. This example is re-used in the paper as a way to easily visualize and check that the defined complexity measures are coherent with one another. The colors on Figure 1b were obtained with a KMeans clustering algorithm applied on the compressed length of the automata states.

As visible on Figure 1b, rules are clearly separated into several clusters that turn out to match Wolfram's classification of ECA. Class 3 behavior can be found at the top of the plot (highest compressed length, orange and blue clusters), Class 1 and 2 are clearly separated at the bottom part (not detailed here) and Class 4 rules (colored in green) lie in between the other types of behavior. The 6 highest scoring rules are shown on Figure 1a and correspond to Class 3 behavior in Wolfram's classification. Among the classes of behavior, some sub-clusters can be found that correspond to similarly behaving rules.

Ultimately, the theoretical goal of using compression algorithms is to approach the theoretical minimum description length of the input [30]. For very regular inputs, this length should be relatively small and inversely for random inputs. However, gzip and PAQ are crude approximations of the minimum description length, and may only approach it in a given context. As an example, compressing text data (a task often performed with gzip in practice) is much more efficient with a language model that can assign a very low probability to non grammatically correct sentences. The Kolmogorov complexity [31] of a cellular automaton is upper bounded by a value that is independent of the chosen rule, as it is entirely determined by the transition table, the grid size, initial configuration and number of steps.

IV. PREDICTOR-BASED METRIC

One obvious limit of using compression length as a proxy for complexity is the fact that interesting systems mostly have intermediate compressed length. Compressed length increases with the amount of disorder in the string being compressed. Therefore, extreme lengths correspond either to systems that do not increase in complexity on the lower end of the spectrum, or systems that produce a maximal amount of disorder on the higher end. Neither of them have the potential to create interesting behavior and increase in complexity. Intermediate values of compressed length are also hard to interpret, since average lengths might either correspond to interesting rules or slowly growing disordered systems.

To cope with this limitation, one should also take into account the dynamics of complexity, that is how the system builds on its complexity at a given time as it keeps evolving, while retaining some of the structures it had acquired earlier. Compression leverages the amount of repetitions in inputs to further compress and this may also be used as an estimate of structure overlap, as explained in the following section.

A. Joint compression

As a way to both measure the complexity and the amount of overlap between two automata states apart in time, we define a joint compressed length metric for a delay τ as

$$C'\left(S^{(T+\tau)}, S^{(T)}\right) = C\left(S^{(T)} \,\|\, S^{(T+\tau)}\right) \tag{2}$$

where $\|$ represents the concatenation operator. This quantity is simply the compressed length of a pair of global states — defined at the beginning of III, represented by the letter S — at two timesteps separated by a delay τ. In 1D, concatenation means chaining the two string representations before compressing, and in 2D we can chain two flattened representations of the 2D grid. This introduces several issues which we discuss in Section IV-B.

To quantify the amount of overlap between the two global states, we can compute the ratio of this joint compressed length with the sum of the two compressed lengths $C(S^t)$ and $C(S^{t-\tau})$, thereby forming the joint compression score

$$\mu = \frac{C\left(S^t\right) + C\left(S^{t-\tau}\right)}{C'\left(S^t, S^{t-\tau}\right)} \tag{3}$$

defined for an automaton S, time t and delay τ.

This metric is based on the intuition that if patterns occur at step $T-\tau$ of the automaton's evolution and are still present at step T, the joint compressed length will be lower than the sum of the two compressed length. The idea is illustrated in Figure 2, where it is pointed out that a stable moving structure (sometimes called *glider* or *spaceships* in Game of Life) will yield lower joint compressed lengths. This also applies to structures that self-replicate, grow from a stable seed or maintain the presence of some sub-structures. Bigger structures yield a higher compression gain.

Joint compression alone is not sufficient since it only selects rules that either behave like identity or shift input because they maximize the conservation of structures through time — as
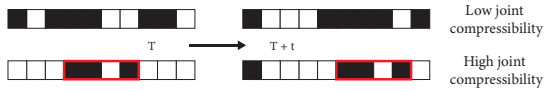
Fig. 2. Joint compression method illustration. If a structure persists through time, this will decrease the joint compressed length compared to the sum of compressed lengths. A persistent structure is circled in red.

illustrated in Figure 3a. However, one may combine the joint compression score with another complexity measure to only select rules that exhibit some disorder, or growth in complexity — as Figure 3b shows (the condition here was a threshold on the difference of compressed length between initial and final states).

(a) Highest joint compression score among the 256 ECA.
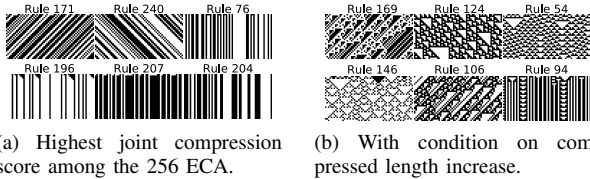
(b) With condition on compressed length increase.

Fig. 3. Comparison of the raw joint compression score and the addition of a complexity increase condition. The high overlap in structures is not enough to get interesting rules a shown in 3a, but the addition of a complexity threshold allows to retrieve rules with complex but still structured behavior, as shown in 3b. Figures are from the same slice of 60 cells over 30 timesteps taken from larger automata with random initial states. The top row corresponds to $t = 0$ and time increases downwards.

B. Count-based predictor

A major issue with the joint compression metric is the fact that it is designed to compress a linear stream of data. This is not ideal when considering higher dimensional automata. Larger sets of transformations have to be considered such as translations, rotations, flips, etc. Theoretically this should not be a problem for a good enough linear compression algorithm, but hardware and software limitations make it impractical to work with existing algorithms on higher dimensional structures — with e.g DEFLATE's upper limit on dictionary size.

These higher dimensional automata might be better at generating complex dynamics, and the large size of their rule spaces makes it a challenge to explore. There has been at least one attempt to deal with these higher dimensional systems [25] that lacks the scalability to work with large inputs.

An alternative to the linear compression-based method presented above would be to use compressors optimized for n-dimensional data (e.g. PNG compression for 2D automata) to take advantage of spatial correlation for compressing. However, these compressors are rare for higher dimensional data, and are usually optimized for one type of input — e.g. images with PNG.

Another way to tackle the problem is to use a prediction based approach to compression. Similarly to methods described in [32] and one of the first steps of the PAQ compression algorithm [19], we learn a statistical model of input data to predict the content of a cell given its immediate predecessors. For compression, this is often followed by an encoding step — using Huffman or arithmetic coding —

that encodes data which contains the least information (least "surprising" data) with the most compact representation. This approach can also be related to the texture synthesis method described in [33], where the authors learn a non parametric model to predict the next pixel of a texture given a previously synthesized neighborhood. Additionally, because we don't need the operation to be reversible as in regular compression, it is not necessary to limit the prediction model to making prediction with predecessors only.

For a global state $S = (c_1, ...c_i, ..., c_n)$, the neighborhood of cell i with radius r, denoted $n_{r,i}$ is defined as the tuple $n_{r,i} = (c_{i-r}, ...c_{i-1}, c_{i+1}..., c_{i+r})$ — without the middle cell. The goal of this method is to estimate the conditional probability distribution $p(s|n_r)$ of the middle states at timestep T given a neighborhood of radius r. Assuming cell states given their neighborhood can be modeled by mutually independent random variables, the log-probability of global state $S^{(T)}$ is written

$$\log p(S^{(T)}) = \log \prod_{i=1}^{N} p(c_i|n_{r,i}) = \sum_{i=1}^{N} \log p(c_i|n_{r,i}) \quad (4)$$

If the automaton has a very ordered behavior, a model will predict with high confidence the state of the middle cell given a particular neighborhood. On the other hand, in the presence of maximal disorder, the middle cell will have an equal probability of being in every state no matter the neighborhood. In the latter case, a predictive model minimizing $-\log p(S^{(T)})$ would yield a high negative log-probability.

A simple possible predictor for such purpose is a large lookup table that maps all visited neighborhoods to a probability distribution over the states that the middle cell can be in. State distributions for each neighborhood are obtained by measuring the frequency of cell states given some observed neighborhoods. We denote by Λ this lookup table, defined for a window of radius r, which maps all possible neighborhoods of size $2r+1$ (ignoring the middle cell) to a set of probabilities p over the possible states $\{s_1, ..., s_n\}$, and p can be written $[p_{s_1}, p_{s_2}, ..., p_{s_n}]$. Λ is defined by

$$\Lambda: \quad \begin{aligned} \{s_1, ..., s_n\}^{2r} &\to \quad \Delta_n \\ n_{r,i} &\mapsto \quad p \end{aligned} \quad (5)$$

where Δ_n denotes the probability simplex in dimension n.

To measure the uncertainty of that predictor, we can compute the cross-entropy loss between the data distribution it was trained on and its output. We compute the log probability of the observed data given the model, or the quantity

$$L = -\frac{1}{N} \sum_{i=1}^{N} \sum_{k=1}^{n} \mathbb{1}_{\{s_k\}}(c_i) \log \Lambda(n_{r,i})_{s_k} \quad (6)$$

where $\mathbb{1}_{\{s_k\}}$ denotes the indicator function of the singleton set $\{s_k\}$. An illustration of the counting process is represented in Figure 4. The quantity L is minimal when the $\Lambda(n_{r,i})_{s_k}$ always equal one, which means the state of every cell is entirely determined by its neighborhood.

We apply this metric to all 256 ECA, with a window radius of size 3 (the 6 closest neighbors are used for prediction), and the same settings as for Figure 1b. Cross-entropy loss of
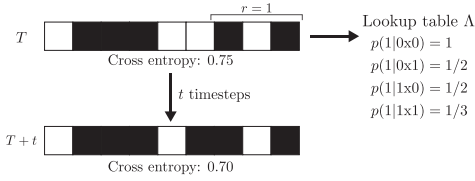
Fig. 4. Count-based predictor method for a radius $r = 1$. A frequency lookup table is computed from the global state at time T by considering all neighborhoods with radius $r = 1$ (3 consecutive cells but ignoring the middle cell). Cross-entropy with the automaton at time T quantifies the overall complexity. This can be compared to the cross-entropy at time $T + t$ for the amount of overlap.

the lookup table gives the results of Figure 5a. Colors are the same as in Figure 1b for comparison purposes.

(a) Count-based predictor
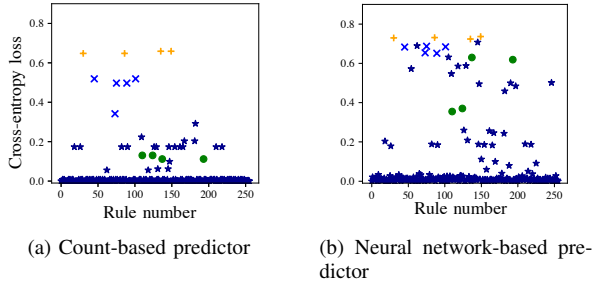
(b) Neural network-based predictor

Fig. 5. Average cross entropy loss for the two predictor-based methods on all 256 ECA. Rules are separated in several clusters. The count-based predictor (left plot) and neural network-based predictor (right plot) were applied with a neighborhood radius $r = 1$ and 3.

We note the similarity between this plot and the one from Figure 1b, with a roughly equivalent resulting classification of ECA rules, with the exception of rules with low score. Rules that produce highly disordered patterns are on top of the plot whereas the very simply behaving rules are at the bottom. This indicates coherence between the two metrics.
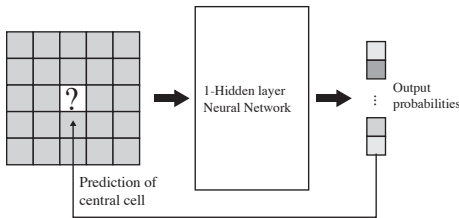
C. Neural network based predictor

Fig. 6. Neural network architecture for predicting a central cell given its neighbors. Output probabilities are defined for all possible states of the central cell.

The frequency based predictor described above still has limitations:

- It doesn't take into account any redundancy in the input which may lead to suboptimal predictions (in a CA, very similar positions might have similar center cell state distribution, e.g. a glider in Game of Life should be recognized by the model no matter the rest of the neighborhood).

- For the same reasons, when considering large window sizes, the number of possible neighborhood configuration gets much larger than the number of observed ones, leading to an input sparsity problem.

More sophisticated models can cope with above limitations by dealing with high dimensional inputs without sparsity problems, and taking into account redundancy of inputs and potential interactions between states for prediction.

We measure the cross-entropy loss of this simple model on the training set after a standard learning procedure which is the same for all rules. The procedure is applied to a one hidden layer neural network with a fixed hidden layer size. We use a ReLU non-linearity for the hidden layer and a softmax to obtain the output probabilities.

For n possible states $s_1, ..., s_n$, a cell in state s_k is represented as a vector of 0s of size n with a 1 in position k. The input to the network is the concatenation of these cell vectors for all cells in the neighborhood. The output of the network is a vector of size n with the output probability for each state.

Gradient updates are computed during training to minimize the cross-entropy loss between outputs and target examples. For a timestep T, we use the training procedure in order to minimize with respect to θ the following quantity,

$$L_\theta^{(T)} = -\frac{1}{N} \sum_{i=1}^{N} \sum_{k=1}^{n} \mathbb{1}_{\{s_k\}} \left(c_i^{(T)} \right) \log \left[f_\theta \left(n_{r,i}^{(T)} \right)_{s_k} \right] \quad (7)$$

where the neural network depending on parameter θ is denoted f_θ, and $n_{r,i}^{(T)}$, the neighborhood of cell i with radius r at time T is defined in the same way as in eq. (6). Loss is computed with respect to the testing set at time $T + \tau$ by computing the same quantity at this subsequent timestep.

The training procedure is selected to achieve reasonable convergence of the loss for the tested examples. It must be well defined and stay the same to allow for comparison of the results across several rules. Score at timestep T for a delay τ is computed with the following formula

$$\mu_\tau = \frac{L^{(T)}}{L^{(T+\tau)}} \quad (8)$$

where $L^{(T+\tau)}$ is the log probability of the automaton state at timestep $T + \tau$ (defined in eq. (7)) according to a model with parameters learned during training at timestep T and $L^{(T)}$ is the same as in eq. (7). The value μ_τ will be lower for easily "learnable" global states that do not translate well in future steps — they create more complexity or disorder — thereby discarding slowly growing very disordered structures. Higher values of μ_τ correspond to automata that have a disordered global state at time T that can be transposed to future timesteps relatively well. Those rules will tend to have interesting spatial properties — not trivially simple but not completely disordered because the model transposes well — as well as a large amount of overlap between a given step and the future ones, indicating persistence of the spatial properties from one state to another. We also selected the metric among other quantities computed from $L^{(T)}$ and $L^{(T+\tau)}$ because it yielded the best score on our experimental datasets.

TABLE I
EXPERIMENTAL RESULTS - AP SCORES

Neural network	$r = 1$	2	3	4	5
5 steps	0.387	0.448	**0.541**	0.525	0.534
50 steps	0.377	0.433	0.517	0.491	**0.542**
300 steps	0.358	0.454	0.488	**0.527**	0.525
Lookup table	$r = 1$	2			
5 steps	0.092	0.070			
50 steps	0.102	0.070			
300 steps	0.093	0.069			

This table shows the average precision (AP) scores obtained on the dataset of section V with the neural network-based and lookup table-based methods. Results are show for delays $\tau = 5, 50, 300$ and several radii values r.

TABLE II
EXPERIMENTAL RESULTS - ACCURACY

Metric	Baseline	Compressed length [20]	Lookup Table	Neural network
Accuracy	0.90	0.913	0.926	**0.953**

Accuracy of each metric of complexity when used to classify which automatons do evolve interestingly, compared against the trivial all-negative baseline and the compressed length metric [20].

V. EXPERIMENTS

We carried out several experiments on a dataset of 500 randomly generated 3 states ($n = 3$) rules with radius $r = 1$. Those rules were manually annotated for interestingness, defined as the presence of visually detectable non trivial structures. The dataset contains 46 rules labeled as interesting and 454 uninteresting rules. Ranking those rules with the metrics introduced above allows to study the influence of parameters and the adequacy between interestingness as we understand it and what the metric measures.

The task of finding interesting rules can either be framed as a classification problem or a ranking problem with respect to the score we compute on the dataset. The performance of our metric can be measured with usual evaluation metrics used on these problems, and notably the average precision (AP) of the resulting classifier.

Average precision scores for the neural network and count-based methods for time windows of 5, 50 and 300 timesteps are given in Table I. Scores were computed on automata of size 256×256 cells, ran for 1000 timesteps ($T + \tau = 1000$). Scores were computed for radii ranging from 1 cell (8 nearest neighbors) to 5 cells (120 neighbors), with a one layer neural network containing 10 hidden units trained for 30 epochs with batches of 8 examples. Best AP for each time window is shown in bold. Results for the frequency lookup table predictor are only shown for $r = 1, 2$ because of sparsity issues with the lookup table from $r = 2$ and above making it unpractical to use the table — 3^{24} possible entries for the lookup table with $r = 2$ against only 256^2 observed states.

From these experiments, bigger radii appear to perform slightly better, although not in a radical way. Since the number of neighbors scales with the square of the radius, reasonably small radii might be a good trade-off between performance and computational cost of the metric.

We also study the performance of our metrics — lookup table and neural network-based — as inputs of a binary classifier against two simple baselines on a random 70/30 split of our dataset. The first baseline classifies all example as negative. The second baseline is based on compressed length as defined in [20] and computed by choosing a pair of thresholds that minimize mean square error when classifying examples in between as positive — this is based on the observation made in Section III that interesting rules have

intermediate compressed lengths. Results are in Table II where only the best radius is shown. The lookup table performs better than the baselines but the neural network gives the best score.

Above experiments demonstrate the capability of our proposed metric to match a subjective notion of interestingness of our labeling. For instance, the top 5 and top 10 scoring rules of the best performing configuration ($r = 3$, $\tau = 5$) are all labeled as interesting, and top 100 scores contain 41 of the 46 rules labeled as interesting.

VI. DISCUSSION

In this section, we discuss the results obtained by using the metric of equation (8) and the way they can be interpreted.

a) One dimensional cellular automata: By applying the metric on the same example as before, we again obtain a plot with a rule classification that matches a visual appreciation of complexity of 1D CA. Results are shown on Figure 5b. Similarly to the previous cases, rules we might label as interesting are unlikely to be either at the top or bottom of the plot.

b) Two dimensional cellular automata: Simulations conducted with 2D CA used grids of size 256×256. Automata were ran for 1000 steps (the metric is measured with respect to the reference time $T = 1000$). Rules are defined with a table of transitions from all possible neighborhood configurations with radius $r = 1$ (3×3 squares) to a new state for the central cell. Unbiased sampling of rules, obtained by uniformly sampling the resulting state for each transition independently, overwhelmingly produces rules with a similar amount of transitions towards each state and fails to produce rules without completely disordered behavior more than 99% of the time.

Therefore, we adopt a biased sampling strategy of the rules, selecting the proportion of transitions towards each state uniformly on the simplex — e.g for 3 states we might get the triple $(0.1, 0.5, 0.4)$ and sample transitions according to these proportions. This parametrization can be related to Langton's lambda parameter [15] that takes into account the proportion of transitions towards a transient (inactive) state and all the other states. We obtain approximately 10% interesting rules with this sampling as the proportions of our experimental dataset show.

Using the neural network-based complexity metric, we were able to find rules with interesting behavior among a very large set through random sampling. Some of these rules are shown in the paper. Figure 8 displays three 2D rules that were selected manually upon visual inspection among the 20 highest scoring for metric μ_{50} (defined in eq. (8)) of a sample
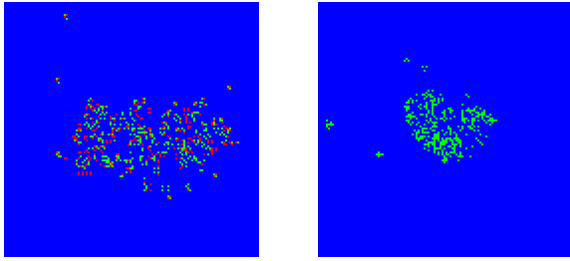
Fig. 7. Rules with 3 states that have spontaneously occurring glider structures. The gliders are the small structures that are outside of the center disordered zone. Some of them move along the diagonals while some others follow horizontal or vertical paths. Note that some repeating patterns occur also in the more disordered center zone.
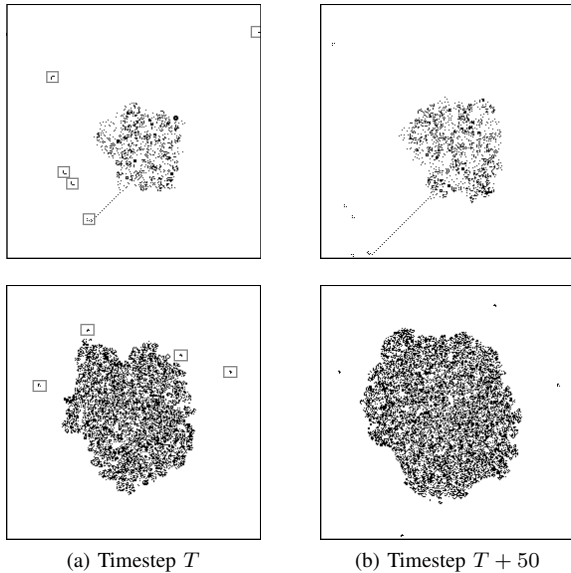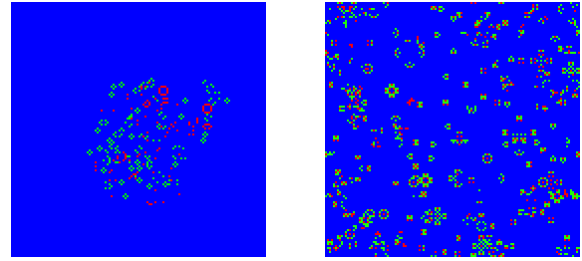

Fig. 9. Rules with 3 states that generate cell-like interacting structures. These patterns are either static or moving and can interact with one another to generate copies of themselves and other patterns. Note the very similar micro-structures that are repeated at several places in the space.

(a) Timestep T (b) Timestep $T + 50$

Fig. 8. Spontaneous glider formation and evolution is observed for some high scoring 2 states rules. Each row corresponds to a rule, with a 50 timesteps difference between the two columns. Gliders are marked with a gray square. Runs were initialized with a small 20 by 20 disordered square (uniformly sampled among possible configuration) in the center simulated for up to 400 steps.
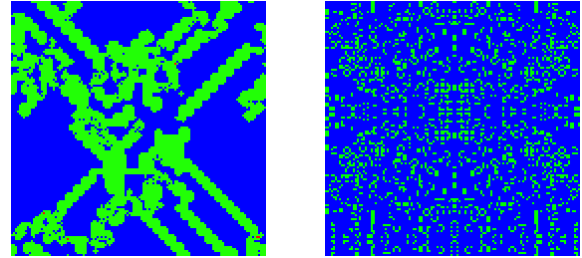

Fig. 10. Rules with surprising behaviors that are highly structured but complex. Those rules were selected among high-ranking rules for the neural-network based complexity metric. They all exhibit structurally non trivial behavior.

of 1700 randomly generated 2-states 3 by 3 neighborhood rules. For comparison, Conway's Game of Life rule (GoL) ranks in the top 1% of the 2500 rules mentioned above for runs that don't end in a static global state. We observe that spontaneous glider formation events appear to be captured by our metric. Although gliders in cellular automata are a simple process that can manually be created, detection of their spontaneous emergence within a random search setting is a first step towards finding more complex macro structures that can emerge out of simple components. Rules with low scores are overwhelmingly of the disordered kind.

Figures 7, 9 and 10 show some three states rules that were selected through random sampling on the simplex with the neural-network based metric. They were selected among the 30 highest scoring rules out of 2500 randomly selected 3 states rules. Their behaviors all involve the growth and interaction of some small structures made of elementary cells.

All automata were initialized with a random disordered square of 20 by 20 cells in the center. In the Figures mentioned above, colors were normalized with the most common state set to blue. Figure 7 shows rules that spontaneously emit gliders that go through space in a direction until they interact with some other active part of the automaton. Figure 9 shows rules that generate small structures of between four and thirty cells that are relatively stable and interact with each other. These elementary components could be a basis for the spontaneous construction of more complex and bigger components. Figure 10 shows some other rules from this set of high ranking automata. They highlight the wide range of behaviors that can be obtained with these systems. Interesting rules from this paper can be found, along with other examples, in the form of animated GIFs[1].

For some of these rules interesting patterns appear less frequently in smaller grids, indicating that the size of the space might impact the ability to generate complex macro-structures. Increasing the size of the state space to very large grids might therefore make it easier generating very complex patterns.

VII. CONCLUSION

In this paper, we have proposed compression-inspired metrics for measuring a form of complexity occurring in complex systems. We demonstrated its usefulness for selecting CA rules that generate interesting emergent structures from very large sets of possible rules. In higher dimensions where linear compression — as in gzip — is not sufficient to find complex patterns, our metric is also useful.

[1]https://bit.ly/interesting_automata

We study 2 and 3 states automata in the paper and we plan to investigate the effects of additional states or larger neighborhoods on the ability to evolve more structures and obtain more interesting behaviors.

In the future, we will publish the dataset and code to enable reproducibility and improvement on the results reported here[2]. The metrics we introduce in this paper could be used to design organized systems of artificial developing organisms that grow in complexity through an evolutionary mechanism. A possible path toward such systems could start by creating an environment where computational resource allocation favors the fraction of subsystems that perform the best according to our measure of complexity.

The proposed metric is theoretically applicable to any complex system where a notion of state of an elementary component and locality can be defined. With these requirements fulfilled, we can build a similar prediction model that uses information about local neighbors to predict the state of a component and thereby assess the structural complexity of an input.

We believe that the capability of creating evolving systems out of such elementary components and with few assumptions could be a step towards AGI. By devising ways to guide this evolution in a direction we find useful, we would be able to find efficient solution to hard problems while retaining adaptability of the system. It might be suitable to avoid over-specialization that can happen in systems designed to solve a particular task — e.g. reinforcement learning algorithms that can play games, and supervised learning — by staying away from any sort of objective function to optimize and by leaving room for open-ended evolution.

References

[1] T. Mikolov, A. Joulin, and M. Baroni, "A roadmap towards machine intelligence," in *International Conference on Intelligent Text Processing and Computational Linguistics*. Springer, 2016, pp. 29–61.

[2] L. Booker, "Perspectives on Adaptation in Natural and Artificial Systems," in *Proceedings Volume in the Santa Fe Institute Studies in the Sciences of Complexity.*, New York, NY, USA, 2004.

[3] T. S Ray, "An approach to the synthesis of life," in *Artificial Life II*, 1st ed., Jan. 1991, pp. 371–408.

[4] K. Sims, "Evolving virtual creatures," in *SIGGRAPH*, 1994.

[5] C. Ofria and C. O. Wilke, "Avida: a software platform for research in computational evolutionary biology," *Artificial Life*, vol. 10, no. 2, pp. 191–229, 2004.

[6] L. Yaeger, "Computational genetics, physiology, metabolism, neural systems, learning, vision, and behavior or Poly World: Life in a new context," in *Santa Fe Institute studies in the Sciences of Complexity*, vol. 17, 1994, pp. 263–263.

[7] A. Channon, "Improving and still passing the ALife test: Component-normalised activity statistics classify evolution in Geb as unbounded," *Proceedings of Artificial Life VIII, Sydney*, pp. 173–181, 2003.

[8] L. Spector, J. Klein, and M. Feinstein, "Division Blocks and the Open-ended Evolution of Development, Form, and Behavior," in *Proceedings of the 9th Annual Conference on Genetic and Evolutionary Computation*, ser. GECCO '07, 2007, pp. 316–323.

[9] L. B. Soros and K. Stanley, "Identifying Necessary Conditions for Open-Ended Evolution through the Artificial Life World of Chromaria," in *Artificial Life 14: Proceedings of the Fourteenth International Conference on the Synthesis and Simulation of Living Systems*, 2014.

[10] D. Pathak, C. Lu, T. Darrell, P. Isola, and A. A. Efros, "Learning to Control Self-Assembling Morphologies: A Study of Generalization via Modularity," in *NeurIPS*, 2019.

[11] J. Von Neumann and A. W. Burks, "Theory of self-reproducing automata," *IEEE Transactions on Neural Networks*, vol. 5, pp. 3–14, 1966.

[12] S. Wolfram, "Universality and complexity in cellular automata," *Physica D: Nonlinear Phenomena*, vol. 10, no. 1, pp. 1–35, Jan. 1984.

[13] N. H. Packard and S. Wolfram, "Two-dimensional cellular automata," *Journal of Statistical Physics*, vol. 38, no. 5/6, 1985.

[14] W. Li, N. H. Packard, and C. G. Langton, "Transition phenomena in cellular automata rule space," *Physica D: Nonlinear Phenomena*, vol. 45, pp. 77–94, 1990.

[15] C. G. Langton, "Computation at the edge of chaos: Phase transitions and emergent computation," *Physica D: Nonlinear Phenomena*, vol. 42, no. 1-3, pp. 12–37, Jun. 1990.

[16] ——, "Self-reproduction in cellular automata," *Physica D: Nonlinear Phenomena*, vol. 10, no. 1, pp. 135–144, Jan. 1984.

[17] E. Bilotta, P. Pantano, and S. Vena, "ARTIFICIAL MICRO-WORLDS PART I: A NEW APPROACH FOR STUDYING LIFE-LIKE PHENOMENA," *International Journal of Bifurcation and Chaos*, vol. 21, no. 02, pp. 373–398, Feb. 2011.

[18] A. Lempel and J. Ziv, "On the Complexity of Finite Sequences," *IEEE Transactions on Information Theory*, vol. 22, no. 1, pp. 75–81, Jan. 1976.

[19] M. V. Mahoney, "Fast Text Compression with Neural Networks," in *FLAIRS*, 2000.

[20] H. Zenil, "Compression-Based Investigation of the Dynamical Properties of Cellular Automata and Other Systems," *Complex Systems*, vol. 19, no. 1, 2010.

[21] H. Zenil and E. Villarreal-Zapata, "Asymptotic behavior and ratios of complexity in cellular automata," *International Journal of Bifurcation and Chaos*, vol. 23, no. 09, 2013.

[22] H. Zenil, "What Is Nature-Like Computation? A Behavioural Approach and a Notion of Programmability," *Philosophy & Technology*, vol. 27, no. 3, pp. 399–421, Sep. 2014.

[23] C. H. Bennett, "Logical Depth and Physical Complexity," in *The Universal Turing Machine A Half-Century Survey*, R. Herken and R. Herken, Eds., Vienna, 1995, vol. 2, pp. 207–235.

[24] H. Zenil, J.-P. Delahaye, and C. Gaucherel, "Image characterization and classification by physical complexity," *Complexity*, vol. 17, no. 3, pp. 26–42, 2012.

[25] H. Zenil, F. Soler-Toscano, J.-P. Delahaye, and N. Gauvrit, "Two-dimensional Kolmogorov complexity and an empirical validation of the Coding theorem method by compressibility," *PeerJ Computer Science*, vol. 1, Sep. 2015.

[26] F. Soler-Toscano, H. Zenil, J.-P. Delahaye, and N. Gauvrit, "Calculating Kolmogorov Complexity from the Output Frequency Distributions of Small Turing Machines," *PLOS ONE*, vol. 9, no. 5, May 2014.

[27] P. Grassberger, "Randomness, Information, and Complexity," in *Proceedings of the 5th Mexican School on Statistical Physics*, 1989.

[28] B. J. LuValle, "The Effects of Boundary Conditions on Cellular Automata," *Complex Systems*, vol. 28, no. 1, pp. 97–124, Mar. 2019.

[29] T. Kowaliw, "Measures of complexity for artificial embryogeny," in *Proceedings of the 10th annual conference on Genetic and evolutionary computation - GECCO '08*. ACM Press, 2008.

[30] P. D. Grünwald, *The minimum description length principle*, ser. Adaptive computation and machine learning, Cambridge, Mass, 2007.

[31] A. N. Kolmogorov, "Three approaches to the quantitative definition of information," *International Journal of Computer Mathematics*, vol. 2, no. 1-4, pp. 157–168, Jan. 1968.

[32] J. Schmidhuber and S. Heil, "Sequential neural text compression," *IEEE Transactions on Neural Networks*, vol. 7, no. 1, pp. 142–146, Jan. 1996.

[33] A. Efros and T. Leung, "Texture synthesis by non-parametric sampling," in *Proceedings of the Seventh IEEE International Conference on Computer Vision*, Kerkyra, Greece, 1999, pp. 1033–1038 vol.2.

[2]https://github.com/hugcis/evolving-structures-in-complex-systems